

# Detection of buried microstructures by nonlinear optical scattering spectroscopy

A. G. F. de Beer<sup>1</sup>, H. B. de Aguiar<sup>1</sup>, J. F. W. Nijssen<sup>2</sup> and S. Roke<sup>1,\*\*</sup>

<sup>1</sup>*Max-Planck Institute for Metals Research,  
70569 Stuttgart, Germany Fax: +49-711-6893612*

<sup>2</sup>*Department of Nuclear Medicine, University Medical Center, Utrecht, The Netherlands*

(Dated: November 6, 2008)

## Abstract

Many processes in chemistry and physics rely on the structure, growth or change of material buried in solids. The impenetrable surrounding medium often prohibits the study of such material in-situ. Nonlinear light scattering can be used to observe the internal structure of a crystalline state embedded inside another solid state. Vibrational sum frequency scattering patterns of polymer microspheres, consisting of both amorphous and crystalline material, reveal the size of the buried micro-structure and the optical components of the second-order susceptibility of the material. The vibrational spectra reveal the molecular structure.

PACS numbers: 42.65.-k, 81.70.Fy, 61.46.+w, 61.18.-j, 61.41+e, 78.67.Bf

---

\*Electronic address: roke@mf.mpg.de

Second-order nonlinear optical experiments are specifically suited to probe molecular properties of buried interfaces and ordered structures (see e.g. [1–5]), since the signal strength is determined by the second-order nonlinear susceptibility  $\chi^{(2)}$ . Equivalent to experiments of macroscopically flat interfaces, second-order Nonlinear Light Scattering (NLS) has recently been introduced to probe interfaces of sub-micron sized colloids dispersed in liquids. Second Harmonic (SH) scattering was used to probe electron transitions in dye molecules on particles suspended in liquids first by [6] and later by others as well [7–11], so that adsorption kinetics on particle surface in dispersions could be followed in situ. The use of infrared photons offers the additional advantage to probe vibrational modes which are very sensitive to chemical structures. NLS Spectroscopy (NLSS), in the form of Vibrational Sum Frequency Generation (VSFG) scattering (see Fig. 1a) has until now only been used to probe molecular interfacial structures and solvent/interface interactions on colloidal particles in solution [12–14]. For interfaces of isotropic particles in isotropic bulk media it has been shown that the angle-dependent intensity depends on the scattering geometry, the size of the particle and also the surface second-order susceptibility [12, 15–18]. NLSS has not been applied yet to buried structures in solid materials.

Detecting small buried crystalline domains in amorphous dielectric solids or amorphous defects in crystalline media without cutting open the solid is a formidable challenge owing to the impenetrable nature of a solid material. Ordinary light scattering is not likely to be useful because it is sensitive to refractive index differences. NLS however, can be very sensitive since the contrast is provided by  $\chi^{(2)}$ .

In this Letter NLSS was used to detect nanoscopic crystalline domains embedded in biodegradable polymer microspheres, which are part of a novel scheme to treat an incurable form of liver cancer [19]. The angular intensity distribution allows us to determine the size of the buried micro-structure, the optical components of the second-order susceptibility of the material and, to some extent, where the material is located. The spectral shape reveals the internal molecular structure of the buried domains. This method has allowed us to explain the apparent structural robustness that seems to be crucial in the understanding of the working mechanism of the treatment: In the proposed medicine the crystalline domains form a host matrix for the incorporated medicinal complex [20].

The biodegradable poly-(L-lactic acid) (PLLA) polymer microspheres were prepared by evaporating the chloroform of a water/chloroform/PLLA emulsion, so that spheres were

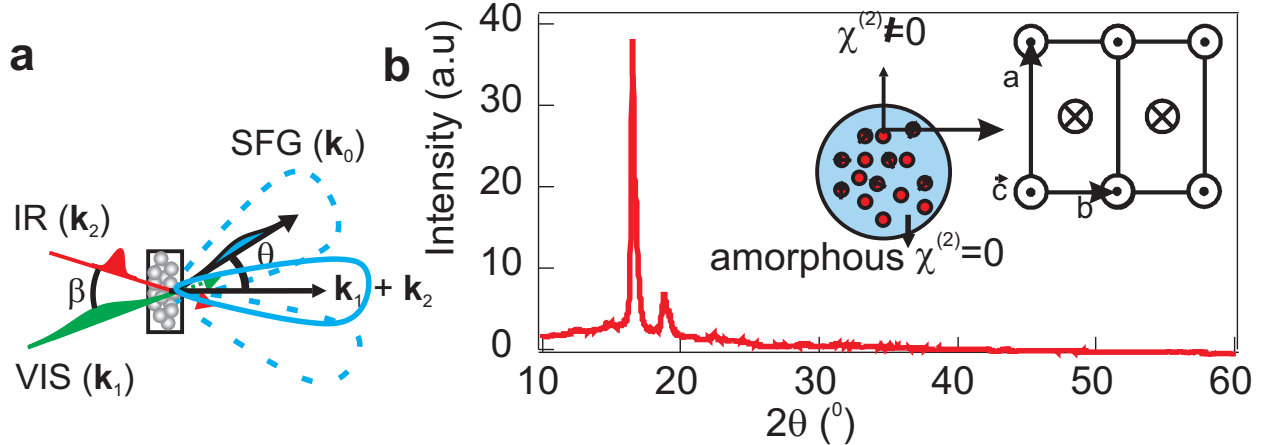


FIG. 1: An illustration of the scattering process. a: IR and VIS laser pulses, with wave vectors  $\mathbf{k}_2$  and  $\mathbf{k}_1$  are incident upon a collection of microspheres. The scattered SFG photons, with wave vector  $\mathbf{k}_0$  are measured in the far field at scattering angle  $\theta$ . The dashed pattern illustrates a typical surface response, whereas the solid pattern originates from buried domains as found in this work. b: XRD pattern of the microspheres. Inset: Illustration of a microsphere consisting of crystalline (red) and amorphous (blue) domains and the  $P2_12_12_1$  crystalline structure of the polymer, poly-(L-lactic acid), with unit axes  $a$ ,  $b$ , and  $c$  [21].

prepared with a broad size distribution of 20 - 50 microns in diameter. The X-ray diffraction pattern in Fig. 1b (recorded with a Philips (Cu-K $\alpha$ 1) diffractometer) reveals the presence of crystalline material. The Bragg reflections are typical for the orthorhombic  $P2_12_12_1$  crystal structure of PLLA, that has two anti-parallel helices per unit cell [22, 23]. The distribution of crystalline material is not known, but the volume fraction was previously estimated at 35 % crystalline material [24, 25]. Although the distribution of crystalline material is not known, the preparation method suggests the presence of isotropically distributed buried domains.

The sum frequency scattering experiments were performed using 7  $\mu\text{J}$  (150 fs) infrared (IR) pulses (repetition rate 1 kHz, FWHM bandwidth of  $\sim 140 \text{ cm}^{-1}$ ) centered around 2995  $\text{cm}^{-1}$  and 3.0  $\mu\text{J}$ , 800 nm visible (VIS) pulses with a 5  $\text{cm}^{-1}$  FWHM bandwidth (see Ref. [26] for more details). The selectively polarized IR and VIS pulses were incident in the horizontal plane under a relative angle of  $15^\circ$  ( $\beta$ ) and focused down to a  $\sim 0.5$  mm beam waist. The scattered light was measured in the same plane and collimated with a lens, polarization selected and spectrally dispersed onto an intensified CCD camera [27]. The

angular resolution was controlled by an aperture placed in front of the collimating lens and was  $5^\circ$ . The microspheres were pressed between two  $\text{CaF}_2$  plates, with a spacing of  $100 \mu\text{m}$ , such that the depth of the sample is at most a few microsphere diameters. Typical recording times were 100 s.

Fig 2 displays the integrated intensity of the scattered sum frequency signal as a function of scattering angle (left panel) as well as 3 spectra obtained at different angles (right panel). The frequency domain spectra recorded at different angles can be described by the absolute

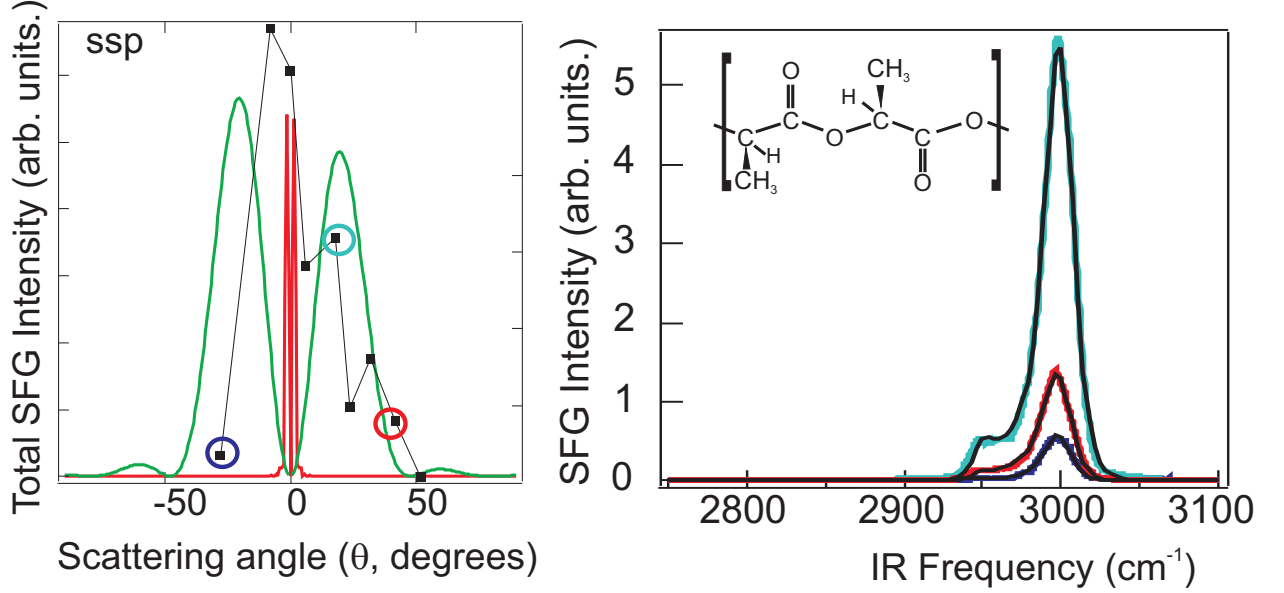


FIG. 2: Intensity pattern and scattering spectra of the microspheres. Left panel: Intensity scattering pattern in the ssp polarization direction from microspheres consisting of amorphous and crystalline domains. A calculated scattering pattern from the outer surface of a microsphere, (red curve, with  $R=20 \mu\text{m}$  and a non-zero surface response  $\chi_{\perp\perp\perp}^{(2)} = 1$ ) and a domain boundary (green curve, with  $R=500 \text{ nm}$  and non-zero surface response  $\chi_{\perp\perp\perp}^{(2)} = 1$ ) are also displayed. Both curves do not describe the data. Right panel: Corresponding frequency domain spectra of the methyl ( $\text{CH}_3$ ) stretch modes for the scattering angles:  $\theta=52^\circ$ ,  $\theta=18^\circ$  and  $\theta=-28^\circ$  (encircled points in the left panel). The monomer unit of PLLA polymer is also shown.

square of the following expression (see e.g. [1, 4, 28]):

$$E_0(\omega) \propto \sum_n \mathbf{E}_2(\omega) \left( A_{nr} e^{i\Delta\phi} + \frac{A_n}{(\omega - \omega_{0n}) + i\Upsilon_n} \right) \otimes \mathbf{E}_1(\omega),$$

where  $A_{nr}$  refers to the non-resonant background with relative phase  $\Delta\phi$ ,  $n$  refers to a vibrational mode, with resonance frequency  $\omega_{0n}$ , amplitude  $A_n$  and damping constant  $\Upsilon_n$ .

Spectrally, the CH<sub>3</sub> groups attached to the helical C-C-O backbone of the PLLA polymer are probed. The spectra resemble those obtained of a crystalline PLLA film [29], and were fit in a global fitting procedure, in which the vibrational modes of the symmetrical (at 2947 cm<sup>-1</sup>) and anti-symmetrical stretch mode (at 2997 cm<sup>-1</sup>) of the CH<sub>3</sub> groups of the polymer chain, together with modes resulting from crystal field splitting [30] (2965 cm<sup>-1</sup> and 3007 cm<sup>-1</sup>) were taken into account. The need to describe the spectra with these 4 modes, indicates that the scattered sum frequency photons could originate from the interior of crystalline domains rather than the surface of the microspheres or the domain boundaries.

Fig. 3 shows the scattering patterns for the most prominent response, the antisymmetrical stretch modes of the CH<sub>3</sub> groups obtained from global fits using Eq. 1 to all spectra recorded at different angles. Plotted is the square modulus of the obtained mode amplitudes as a function of scattering angle  $\theta$  for different polarization combinations. As can be seen from Fig 2a and Fig. 3 the maximum scattered intensity occurs in the forward direction ( $\theta = 0^\circ$ ). This is distinctly different from the result one would expect from a second-order nonlinear scattering experiment from a particle interface (as there is no expected signal in the forward direction). The reason could be that the dominant source of the scattering pattern is the interior (crystalline) domains.

To describe the scattering pattern of an embedded domain we have to consider that at each point ( $\mathbf{r}'$ ) inside the domain a second-order nonlinear polarization ( $\mathbf{P}^{(2)}(\mathbf{r}')$ ) is built up. Because the orientation of the domains is unknown and most likely consist of an isotropic distribution, we assume that the  $a$ ,  $b$ , and  $c$  axes system of each domain is rotated with respect to the laboratory frame with (Euler) angles  $\psi, \xi, \zeta$ . To obtain the scattered field per domain we have to sum over all the positions inside the volume  $V$  of the domain. We can then write for the sum frequency field at the detector (positioned at  $r_0$ ) generated by a single crystallite:

$$\mathcal{E}_{u_0 u_1 u_2}^{(2)}(r_0) \propto \mathcal{E}_{u_1} \mathcal{E}_{u_2} e^{ik_0 r_0} \frac{k_0^2}{r_0} \int_V e^{i\mathbf{q}\cdot\mathbf{r}'} d^3\mathbf{r}' \sum_{\alpha_0, \alpha_1, \alpha_2} \chi_{\alpha_0, \alpha_1, \alpha_2}^{(2)} \prod_{i=0}^2 (\mathcal{R}(\mathbf{e}'_{\alpha_i}) \cdot \mathbf{e}_{u_i}). \quad (1)$$

Here,  $\mathcal{E}$  is the electric field amplitude,  $\mathbf{e}_{u_i}$  is the unit vector for polarization state  $u_i$  of the incoming and outgoing beams,  $k_0$  is the magnitude of the wavevector of the scattered SFG light, and  $\mathbf{q}$  is the scattering wavevector, which is here defined as the difference between the scattered SFG wavevector and the sum of the incoming wavevectors ( $\mathbf{k}_0 - \mathbf{k}_0^0$ ).  $\alpha_i$  represents the orthonormal base for crystalline axes  $a$ ,  $b$  or  $c$ ,  $\mathcal{R}$  represents a rotation over Euler angles

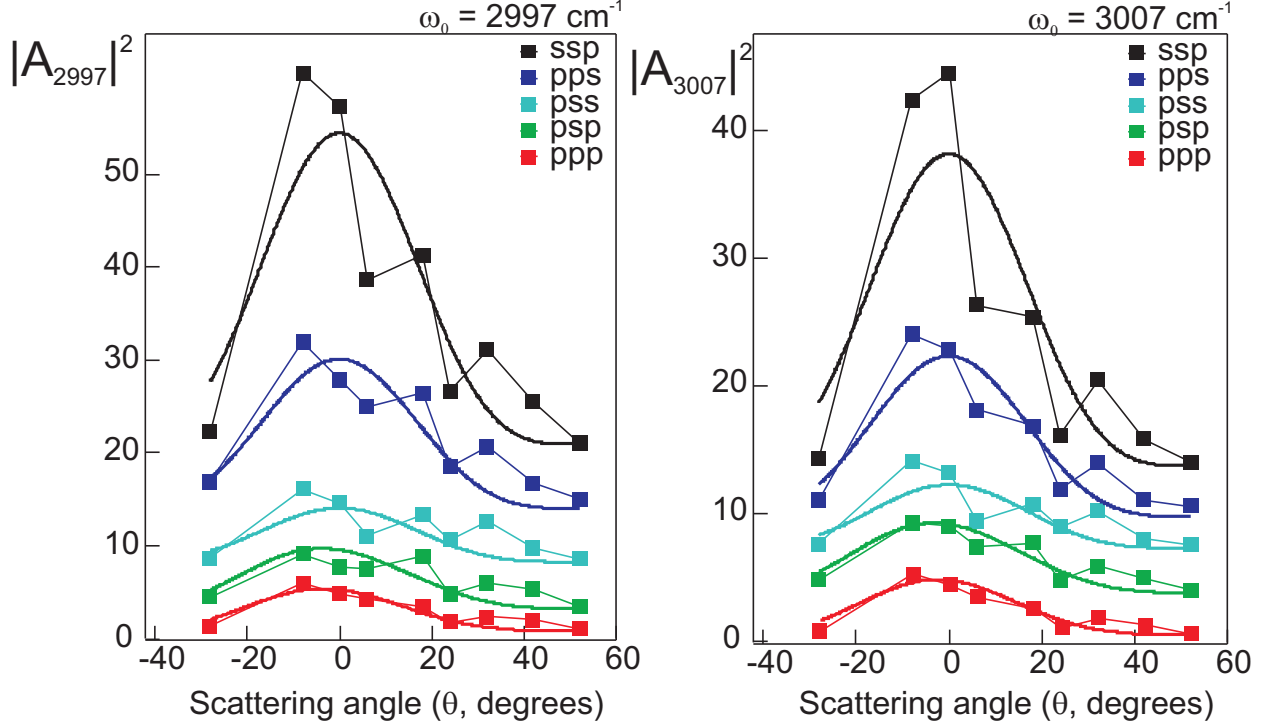


FIG. 3: Scattering patterns from two methyl stretch modes. Plotted is the squared amplitude ( $|A_n|^2$ ) of the vibrational modes of the  $\text{CH}_3$  groups at  $2997 \text{ cm}^{-1}$  (left panel) and  $3007 \text{ cm}^{-1}$  (right panel) for the polarization combinations ssp, pps, pss, ppp and spp. The fits (solid curves) are made with Eqs. 6, using  $R = 565 \pm 29 \text{ nm}$  with  $\chi_{abc}^{(2)} = \chi_{bac}^{(2)} = 0$ ,  $\chi_{cab}^{(2)} = \chi_{acb}^{(2)} = 1.35 \pm 0.74$  and  $\chi_{bca}^{(2)} = \chi_{cba}^{(2)} = 11.17 \pm 1.78$  for  $2997 \text{ cm}^{-1}$  and  $\chi_{abc}^{(2)} = \chi_{bac}^{(2)} = 0$ ,  $\chi_{cab}^{(2)} = \chi_{acb}^{(2)} = 9.99 \pm 1.63$  and  $\chi_{bca}^{(2)} = \chi_{cba}^{(2)} = 0.77 \pm 0.78$  for  $3007 \text{ cm}^{-1}$ .

$\psi$ ,  $\xi$ , and  $\zeta$ , necessary to describe an arbitrarily oriented crystalline domain.  $V$  is the domain volume, and since it is unknown, we approximate the domain shape as spherical (with radius  $R$ ). Since the difference in refractive index between crystalline and amorphous polymer is very small we may use the Rayleigh-Gans-Debye approximation [11, 31, 32]. Away from electronic resonance the space group of crystalline PLLA has the following non-zero susceptibility elements:  $\chi_{abc}^{(2)} = \chi_{bac}^{(2)}$ ,  $\chi_{cab}^{(2)} = \chi_{acb}^{(2)}$ , and  $\chi_{bca}^{(2)} = \chi_{cba}^{(2)}$  [33, 34]. More specifically, for the methyl stretch modes of crystalline poly-(L-lactic acid), it is known that  $\chi_{abc}^{(2)} = \chi_{bac}^{(2)} = 0$  [22]. Because the integration is done over  $\mathbf{r}'$ , which is independent from  $\boldsymbol{\chi}^{(2)}$ , we can split the equation into a domain size dependent part ( $F(qR)$ ) and a part that depends also

on the nonlinear optical properties of the material ( $G(\theta; \psi, \xi, \zeta)$ ):

$$\mathcal{E}_{u_0 u_1 u_2}^{(2)}(r_0) \propto \mathcal{E}_{u_1} \mathcal{E}_{u_2} e^{ik_0 r_0} \frac{k_0^2}{r_0} F(qR) G(\theta; \psi, \xi, \zeta) \quad (2)$$

$$F(qR) = \int_V e^{i\mathbf{q}\cdot\mathbf{r}'} d^3\mathbf{r}' = 4\pi R^3 \frac{\sin(qR) - qR \cos(qR)}{(qR)^3} \quad (3)$$

$$G(\theta; \psi, \xi, \zeta) = \sum_{\alpha_0, \alpha_1, \alpha_2} \chi_{\alpha_0, \alpha_1, \alpha_2}^{(2)} \prod_{i=0}^2 (\mathcal{R}(\mathbf{e}'_{\alpha_j}) \cdot \mathbf{e}_{u_i}). \quad (4)$$

$F(qR)$  appears as a scattering form factor function [31], just like it does in linear scattering and depends on the scattering angle ( $\theta$ ) through  $\mathbf{q}$ . It is symmetric and non-zero around  $\theta = 0^\circ$ . The size of a domain determines how sharp it is peaked. This is in correspondence with what is observed.  $G(\theta; \psi, \xi, \zeta)$  is unique for NLSS and is different for each crystalline domain since it depends on the orientation of the domain compared to the laboratory axis system. For an isotropic distribution of ( $N$ ) domains we have to incoherently sum the light that is generated coherently in each domain. This results in the following equation for the scattered intensity:

$$I_{u_0, u_1, u_2}(r_0) \propto N \mathcal{E}_{u_1}^2 \mathcal{E}_{u_2}^2 \frac{k_0^4}{r_0^2} |F(qR)|^2 \int_0^{2\pi} \int_0^\pi \int_0^{2\pi} \left| \sum_{\alpha_0 \alpha_1 \alpha_2} G(\theta; \psi, \xi, \zeta)_{\alpha_0 \alpha_1 \alpha_2} \right|^2 d\zeta \sin \xi d\xi d\psi. \quad (5)$$

These equations can be evaluated analytically. For domains of crystalline PLLA polymer the resultant equation has the following form:

$$I_{u_0, u_1, u_2}(r_0) \propto N \mathcal{E}_{u_1}^2 \mathcal{E}_{u_2}^2 \frac{k_0^4}{r_0^2} |F(qR)|^2 [(c_1 + c_2 \cos(2\theta) + c_3 \sin(2\theta)) \left( (\chi_{bca}^{(2)})^2 + (\chi_{cab}^{(2)})^2 \right) + (c_4 + c_5 \cos(2\theta) + c_6 \sin(2\theta)) \chi_{bca}^{(2)} \chi_{cab}^{(2)}]. \quad (6)$$

For our non-collinear beam geometry some polarization combinations become complicated expressions. For  $\beta = 15^\circ$  the coefficients ( $c_{1\dots 6}$ ) become (3.6, -0.25, 0.73, 3.8, 1.7, -0.96), (8.7, 0.37, 0.038, -3.8, 0.75, 0.075) and (6.0, -2.1, 0.93, -1.1, 3.1, -1.4) for ppp, pps and psp respectively, while for spp, pss, sps, ssp, and sss they are: (4.0, 0, 0, 1.8, 0, 0), (3.8, 0, 0, 2.3, 0, 0), (3.8, 0, 0, 2.3, 0, 0), (9.0, 0, 0, -3.0, 0, 0), and (3.0, 0, 0, 0, 0, 0), for which the coefficients  $c_2$ ,  $c_3$ ,  $c_5$  and  $c_6$  vanish, so that the angular intensity distribution is determined only by the *size* of the crystalline domains. The best simultaneous fit to all patterns in Fig. 3 yields  $R = 565 \pm 29$  nm, together with the relative  $\chi^{(2)}$  components given in the caption. Only one susceptibility element is large for each mode. The non-zero modes correspond to vibrations with  $B_2$  and  $B_3$  symmetry respectively, and they should indeed be orthogonal [22, 30].

In contrast, scattering from the interface of the boundary domains or the interface of the microspheres (calculated using a surface nonlinear optical response [32, 35] and displayed in Fig. 2) does not match at all with the observed scattering pattern. Further, we observe scattered SFG photons in all 8 polarization combinations. This too is different from a pure surface scattering experiment, in which one expects only 4 polarization combinations to be non-vanishing (see e.g [11, 12, 36]), so that it can be excluded as a (dominant) source of signal. The observed pattern and polarization combinations can be used as a means of locating the source of the scattered photons.

Thus, we can observe the internal structure of a crystalline state embedded inside another solid state. The scattering pattern allows us to determine the size of the buried micro-structure, the optical components of the second-order susceptibility of the material and, to some extent, where the material is located (since segregated crystalline material at the surface would give rise to a distinctly different scattering pattern, and different polarization combinations). Comparing the relative intensity and presence of vibrational modes in the spectra allows one to determine the molecular structure. This method adds to existing methods such as X-Ray Diffraction and light scattering in that molecular structural determination is possible simultaneously with the size and rough location determination. The sizes determined are not the extent of single crystals (as with XRD, which is based on detecting Bragg reflections from crystal planes), but rather the size of an ordered domain (such as a spherulite), which can occur in the range of several nm up to several tens of microns. Also, second-order nonlinear optical signals depend quadratically on the field amplitudes and the efficiency of the process can be resonantly enhanced so that it can be expected that a very low detection limit can be reached [37]. Another difference is the absence of the need of a mismatch in refractive index between the various phases.

The method presented here has already been used successfully to determine that in a variant of these microspheres used for liver cancer treatment, the crystalline domains form a host matrix for the incorporated medicinal complex [20]. This explains the apparent structural robustness that is crucial for understanding the working mechanism of the treatment. We expect therefore that NLSS will be very useful in identifying buried structures in situ and non-invasively in other components as well, with a high sensitivity. New insights can be obtained in many processes in chemistry and physics, such as the monitoring of nucleation and growth processes, the detection of small portions of biological crystals (such as proteins

and biopolymers) and the assembly of matrix based medicines.

This work is part of the research programme of the Max-Planck Society. We thank U. Welzel for providing XRD patterns, and M. Bonn, D. Dlott, R. Vogelgesang, and G. Ertl for comments and discussions.

- 
- [1] T. F. Heinz, *Nonlinear surface electromagnetic phenomena* (Elsevier, New York, 1991), chap. Second-order nonlinear optical effects at surfaces and interfaces, p. 353.
  - [2] Y. R. Shen, *The principles of nonlinear optics* (Wiley, New York, 1984).
  - [3] C. T. Williams and D. A. Beattie, *Surf. Sci.* **500**, 545 (2002).
  - [4] S. Roke, J. M. Schins, M. Müller, and M. Bonn, *Phys. Rev. Lett.* **90**, 128101 (2003).
  - [5] M. S. Yeganeh, S. A. Dougal, and B. G. Silbernagel, *Langmuir* **22**, 637 (2006).
  - [6] H. Wang, E. C. Y. Yan, E. Borguet, and K. B. Eisenthal, *Chem. Phys. Lett.* **259**, 15 (1996).
  - [7] K. B. Eisenthal, *Chem. Rev.* **106**, 1462 (2006).
  - [8] R. K. Campen, D. S. Zheng, H. F. Wang, and E. Borguet, *J. Phys. Chem. C.* **111**, 8805 (2007).
  - [9] H. F. Wang, T. Troxler, A. G. Yeh, and H. L. Dai, *J. Phys. Chem. C* **111**, 8708 (2007).
  - [10] L. Schneider, H. J. Schmid, and W. Peukert, *Appl. Phys. B* **87**, 333 (2007).
  - [11] N. Yang, W. E. Angerer, and A. G. Yodh, *Phys. Rev. Lett.* **87**, 103902 (2001).
  - [12] S. Roke, W. G. Roeterdink, J. E. G. J. Wijnhoven, A. V. Petukhov, A. W. Kleyn, and M. Bonn, *Phys. Rev. Lett.* **91**, 258302 (2003).
  - [13] S. Roke, J. Buitenhuis, J. C. van Miltenburg, M. Bonn, and A. van Blaaderen, *J. Phys.-Condens Matter* **17**, S3469 (2005).
  - [14] S. Roke, O. Berg, J. Buitenhuis, A. van Blaaderen, and M. Bonn, *Proc. Nat. Acad. Sci.* **103**, 13310 (2006).
  - [15] J. I. Dadap, J. Shan, K. B. Eisenthal, and T. F. Heinz, *Phys. Rev. Lett.* **83**, 4045 (1999).
  - [16] J. Shan, J. I. Dadap, I. Stiofkin, G. A. Reider, and T. F. Heinz, *Phys. Rev. A* **73**, 023819 (2006).
  - [17] J. Martorell, R. Vilaseca, and R. Corbalan, *Phys. Rev. A.* **55**, 4520 (1997).
  - [18] N. Yang, W. E. Angerer, and A. G. Yodh, *Phys. Rev. A* **6404**, 045801 (2001).
  - [19] J. F. W. Nijsen, A. D. van het Schip, W. E. Hennink, D. W. Rook, P. P. van Rijk, and J. M. H.

- de Klerk, *Curr. Med. Chem.* **9**, 73 (2002).
- [20] H. B. de Aguiar, J. F. W. Nijssen, and S. Roke, in preparation (2008).
- [21] C. Aleman, B. Lotz, and J. Puiggali, *Macromolecules* **34**, 4795 (2001).
- [22] K. Aou and S. L. Hsu, *Macromolecules* **39**, 3337 (2006).
- [23] S. H. Kang, S. L. Hsu, H. D. Stidham, P. B. Smith, M. A. Leugers, and X. Z. Yang, *Macromolecules* **34**, 4542 (2001).
- [24] J. F. W. Nijssen, B. A. Zonnenberg, J. R. W. Woittiez, D. W. Rook, I. A. Swildens-van Woudenberg, P. P. van Rijk, and A. D. van het Schip, *Eur. J. Nucl. Med.* **26**, 699 (1999).
- [25] J. F. W. Nijssen, M. J. van Steenbergern, H. Kooijman, H. Talsma, L. M. J. Kroon-Batenburg, M. van de Weert, P. P. van Rijk, A. de Witte, and A. D. V. Schip, *Biomaterials* **22**, 3073 (2001).
- [26] A. B. Sugiharto, C. M. Johnson, H. B. de Aguiar, L. Aloatti, and S. Roke, *Appl. Phys. B.* **91**, 315 (2008).
- [27] L. J. Richter, T. P. Petralli-Mallow, and J. C. Stephenson, *Opt. Lett.* **23**, 1594 (1998).
- [28] J. H. Hunt, P. Guyot-Sionnest, and Y. R. Shen, *Chem. Phys. Lett.* **133**, 189 (1987).
- [29] C. M. Johnson, A. B. Sugiharto, and S. Roke, *Chem. Phys. Lett.* **449**, 191 (2007).
- [30] D. I. Bower and W. F. Maddans, *Vibrational spectroscopy of polymers* (Cambridge university press, Cambridge, 1992).
- [31] M. Kerker, *The scattering of light and other electromagnetic radiation* (John Wiley and sons, New York, 1969).
- [32] S. Roke, M. Bonn, and A. V. Petukhov, *Phys. Rev. B.* **70**, 115106 (2004).
- [33] R. W. Boyd, *Nonlinear optics* (Academic Press, New York, 1992).
- [34] X. Zhuang, P. B. Miranda, D. Kim, and Y. R. Shen, *Phys. Rev. B.* **59**, 12632 (1999).
- [35] A. G. F. de Beer and S. Roke, *Phys. Rev. B.* **75**, 245438 (2007).
- [36] J. I. Dadap, J. Shan, and T. F. Heinz, *J. Opt. Soc. Am. B* **21**, 1328 (2004).
- [37] H. B. de Aguiar and S. Roke, in preparation (2008).